Journal of Polymers and the Environment (2025) 33:3013–3028
https://doi.org/10.1007/s10924-025-03592-7

ORIGINAL PAPER

Usage of 3D-Printed Scaffolds Manufactured with Bio-Based Photopolymer Resin Via 3D DLP in Tissue Engineering

Özge Tezel[1] · Memet Vezir Kahraman[1] · Ramazan Ceylan[2,3] · Ayşegül Açıksarı[2] · Ebru Demir[2,3] · Sibel Çetinel[2,3]

Accepted: 9 May 2025 / Published online: 15 May 2025

Abstract

In this study, three-dimensional (3D) printed scaffolds were fabricated using a bio-based photopolymer resin derived from sustainable resources for tissue engineering applications. The resin consisted of a UV-curable bio-based fatty acid-based polyester acrylate, polyethylene glycol dimethacrylate, and a photoinitiator. To enhance porosity and biodegradability, coconut oil and poly(ethylene glycol) (PEG) were incorporated into the formulations. The curing behavior of different formulations was investigated by differential photocalorimetry (Photo-DSC), and it was observed that polyethylene glycol accelerated the curing process. The biocompatibility of the 3D printed scaffolds was evaluated using culture experiments with mouse fibroblast (L-929) cells. The obtained results demonstrate that the developed bio-based photopolymer resins have the potential to be a promising material for tissue engineering applications.

✉ Memet Vezir Kahraman
mvezir@marmara.edu.tr

[1] Faculty of Sciences, Department of Chemistry, Marmara University, 34722 Goztepe, Istanbul, Türkiye

[2] Nanotechnology Research and Application Center (SUNUM), Sabancı University, 34956 Istanbul, Türkiye

[3] Faculty of Engineering and Natural Science (FENS), Sabancı University, 34956 Istanbul, Türkiye

Graphical Abstract

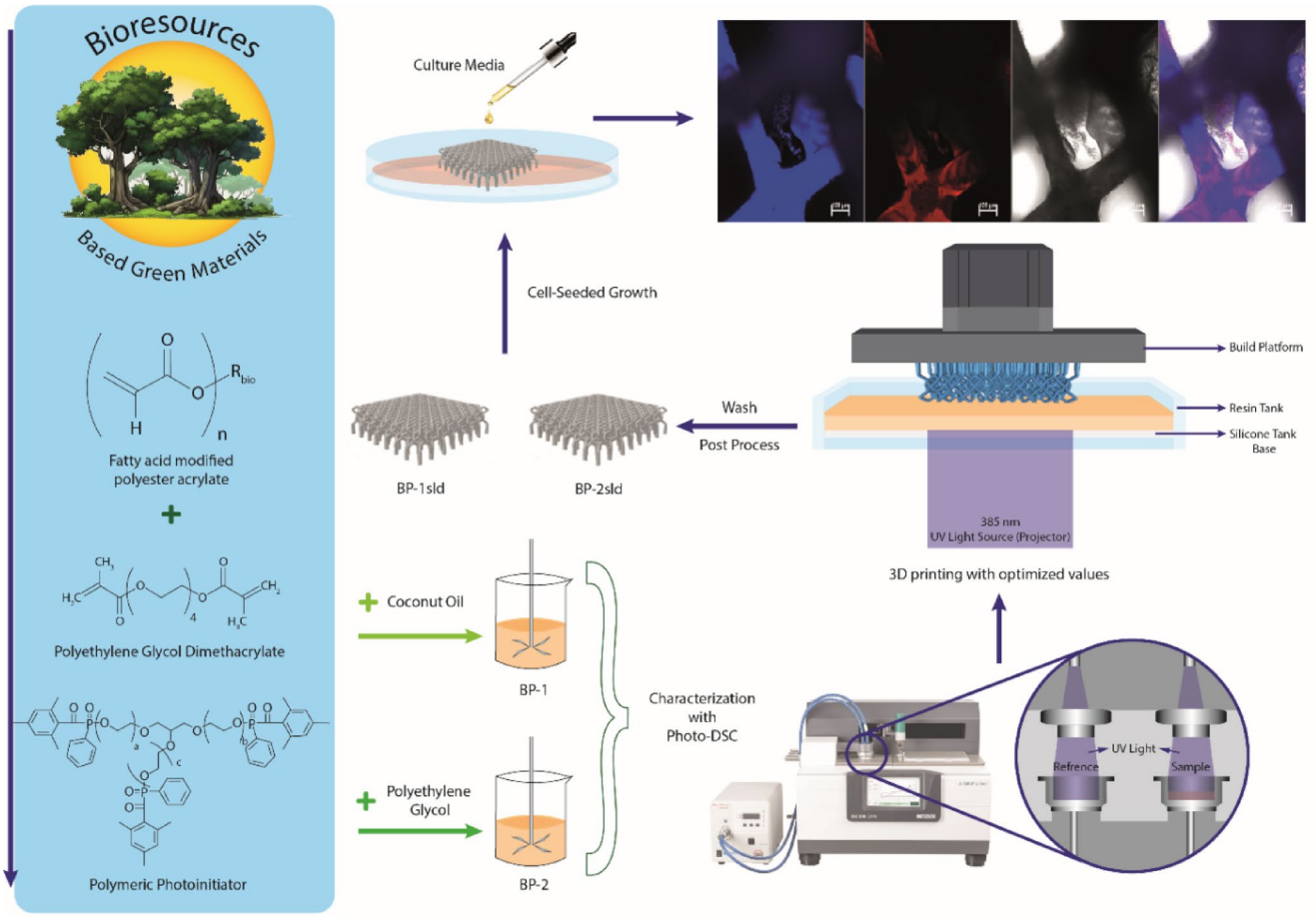

Keywords 3D printing · 3D scaffold · Photo-DSC · Photopolymerization · Fibroblast · Tissue Engineering

1. Introduction

Sustainability has evolved from a mere trend to one of the most critical issues shaping our future. The importance of balancing natural resources with social and economic factors is now more evident than ever. In this context, the interest in bio-based polymers is rapidly increasing, while innovative manufacturing techniques such as additive manufacturing are playing a significant role in this field. The environmental impacts of traditional petrochemical-based plastics have stimulated research and production of bio-based polymers derived from renewable sources such as vegetable oils, cellulose, and lactic acid. Vegetable oils are frequently preferred raw materials in this field due to their low cost and environmental friendliness. Fatty acids, known as triglycerides, can undergo various chemical reactions due to their polyunsaturated structures, resulting in products with different properties. The alkene groups of common vegetable oils such as soybean oil, castor oil, and palm oil can be modified through appropriate reactions to impart functionality to unsaturated alkenes, thus obtaining bio-based acrylic oligomers [1, 2, 3, 4]. These oligomers can then be used in various applications.

On the other hand, additive manufacturing, also known as 3D printing, enables the creation of a physical object by adding layer upon layer. With 3D printers, users can produce only what is needed in a short time by using exactly the amount of material required to create a part or product. This results in savings in energy, time, and materials. 3D printing technology is particularly of great interest in personalized medicine, tissue engineering, and other biomedical applications [5, 6].

Tissue engineering scaffolds used in tissue engineering applications can be defined as three-dimensional and porous structures designed to trigger desired biological responses. These structures support the formation of new tissues by enabling cell adhesion, proliferation, and differentiation. To achieve tissue reconstruction in tissue engineering

applications, scaffolds created using 3D printers must meet certain requirements. It is necessary for the scaffold to have high porosity and sufficient pore size to facilitate cell seeding and nutrient diffusion throughout the entire scaffold structure [7]. In addition, the structure of the tissue scaffold is expected to be biocompatible and biodegradable without having any adverse effects on the cells.

There are many 3D printing technologies developed depending on the properties of the material to be processed and the chemical, physical, and mechanical properties of the final product [8, 9, 10]. Photopolymer resins used in 3D printers operating with stereolithography (SLA) and Digital Light Processing (DLP)/Liquid Crystal Display (LCD) technologies can be converted from liquid to solid when exposed to a specific light source (e.g., UV light), allowing the creation of complex and high-resolution 3D structures. DLP-based 3D tissue scaffold applications can operate with a sensitivity of 32 microns in the x-y axis and 10 microns in the z axis, depending on the capacity of the 3D printer [11]. This means a significantly higher sensitivity, accuracy, and precision than extrusion-based 3D bioprinters.

The curing behavior of photopolymer resins in 3D printing processes directly affects the mechanical properties and biocompatibility of the scaffolds. Factors such as photoinitiator type, polymerization efficiency, chemical structure, and toxicity of photoproducts determine these factors. Conventional small molecule-based photo initiators can create toxic photoproducts that can move within the polymer network after curing and leak into the cell culture medium. This can lead to undesirable biological interactions in tissue engineering applications. The use of polymeric photoinitiators limits the mobility of photoproducts, increasing the biocompatibility of scaffolds and offering a safer alternative for long-term tissue engineering applications [12].

Bioinks containing type 1 Ethyl phenyl(2,4,6-trimethylbenzoyl) phosphinate (TPO-L) photoinitiator developed by Zhaochuang Wang and colleagues can be used in 3D printers operating with DLP technology thanks to the thiol-yne cross-linking mechanism and the fluid nature of prepolymers [13]. These bioinks have great potential for creating personalized and biologically compatible structures in fields such as tissue engineering.

Although DLP technology has significant advantages over other 3D printing technologies, the limited availability of printable photosensitive resins with biocompatibility and biodegradability limits its development in tissue engineering applications [14]. Therefore, researchers have to make different modifications both in the material to be processed and in the 3D printer to be applied. Xiaxia Yang et al. have developed a low-temperature DLP 3D printing technique using low concentrations of Collagen Methacryloyl (ColMA) and Gelatin Methacryloyl (GelMA) to produce durable and bioactive personalized scaffolds due to the difficulties of collagen denaturation at high temperatures and aggregation at neutral pH [15].

In nerve tissue engineering, biomaterial scaffolds with high conductivity and customized structures are very important in supporting nerve regeneration. Ying Han et al. used DLP 3D printing technology in nerve tissue engineering applications to produce complex hydrogel structures by interfacial polymerization to create conductive pathways within a hydrogel structure. Here, they have developed a promising conductive hydrogel with excellent chemical stability and biocompatibility containing Poly(3,4-ethylenedioxythiophene) (PEDOT). The integration of PEDOT has significantly increased the electrical conductivity and mechanical properties of the Gelatin Methacryloyl/Chitosan hydrogel [16].

The combination of bio-based polymers and additive manufacturing creates a significant future to achieve sustainability and personalized production goals. This makes it possible to obtain products that produce less waste, are environmentally friendly, and are biocompatible. In particular, bio-based polymer-based implants and tissue engineering structures in the biomedical field can play an important role in improving patients' quality of life.

This study presents a sustainable and biocompatible approach for producing 3D-printed tissue scaffolds using photopolymer resins derived from natural resources. 3D-printed tissue scaffolds produced using photopolymer resins from natural sources combine the principles of biocompatibility and environmental sustainability. In line with the principles of resource efficiency and waste minimization, Photo-DSC analysis was used to optimize the curing properties of the resins, and high-resolution, non-toxic tissue scaffolds were produced using a DLP 3D printer. To achieve the desired porosity and biodegradability of the tissue scaffolds, polyethylene glycol or coconut oil, derived from renewable sources, were added to the photopolymer formulations and then removed from the system by post-printing washing processes. L-929 fibroblasts were seeded onto the tissue scaffolds, and biocompatibility and cell population were evaluated. Cell culture studies showed the positive effects of the produced scaffolds on cell adhesion and proliferation. These results demonstrate that bio-based photopolymers supported by polyethylene glycol or coconut oil provide an innovative and promising technique in the field of environmentally friendly and sustainable tissue engineering. The main objective of this study is to scientifically demonstrate that the integration of sustainability principles into tissue engineering applications can contribute to both human health and environmental sustainability.

2. Materials & Methods

2.1. Materials

Fatty Acid Modified Polyester Acrylate Sarbio 7201 (S7201, functionality: 6) and Sarbio 7202 (S7202, functionality: 4) (Arkema, France) and Polyethylene Glycol (200) di methacrylate Sarbio 6201 (S6201, functionality: 2) (Arkema, France) were used as acrylate bases of the photopolymer resin. Polymeric photo initiator ethyl(2,4,6-trimethylbenzoyl)-phenyl phosphinate (Omnipol-TP) was purchased from IGM Resins. Poly (ethylene glycol) (average mol wt. 200) (PEG) was supplied from INEOS Chemicals. Coconut oil was obtained from a local herbalist.

To evaluate cytotoxicity, cell adhesion, and proliferation, the mouse fibroblast cell line L929 (ATCC CCL-1) was employed. Cells were cultured in Dulbecco's Modified Eagle Medium (DMEM, PAN Biotech, Germany) supplemented with 10% fetal bovine serum (FBS, Gibco, Thermo Fisher Scientific, UK) and 1% penicillin-streptomycin (Capricorn Scientific, Germany). Cell viability was assessed using the MTT (3-(4,5-dimethylthiazol-2-yl)-2,5-diphenyltetrazolium bromide, neoFroxx, Germany) assay. Cells were seeded in 96-well plates (TPP, Switzerland), and formazan crystals were dissolved in dimethyl sulfoxide (DMSO, neoFroxx, Germany). To prevent cell adhesion to the petri dish, the dish was coated with polydimethylsiloxane (PDMS, Sylgard 184 Silicone Elastomer Kit, Dow Corning Midland, MI). Phosphate-buffered saline (PBS, PAN Biotech, Germany) was used for in situ degradation and washing procedures. Cell proliferation was evaluated using the CCK-8 assay (GlpBio, USA). At the end of the incubation, cells were fixed with paraformaldehyde (PFA, Sigma Aldrich, Germany) and dehydrated with hexamethyldisilazane (HMDS, Sigma Aldrich, Germany).

2.2. Preparation of Biobased Photopolymer Formulations

A bio-based fatty acid modified polyester acrylate (with 45% biorenewable carbon content) was used, along with Polyethylene Glycol di methacrylate to reduce viscosity and enhance printability. A type 1 polymeric photoinitiator, activated at 360–405 nm wavelengths and with a structure shown in Fig. 1.a, was selected. The reason for choosing a polymeric photoinitiator is to extend the active-ended polymer chains in the cross-linking polymer system and to reduce the toxic effects of the photopolymer due to photoinitiator migration [17].

Coconut oil and Polyethylene Glycol were added separately to the formulations of cross-linkable acrylates and the photoinitiator system. This allows for the creation of

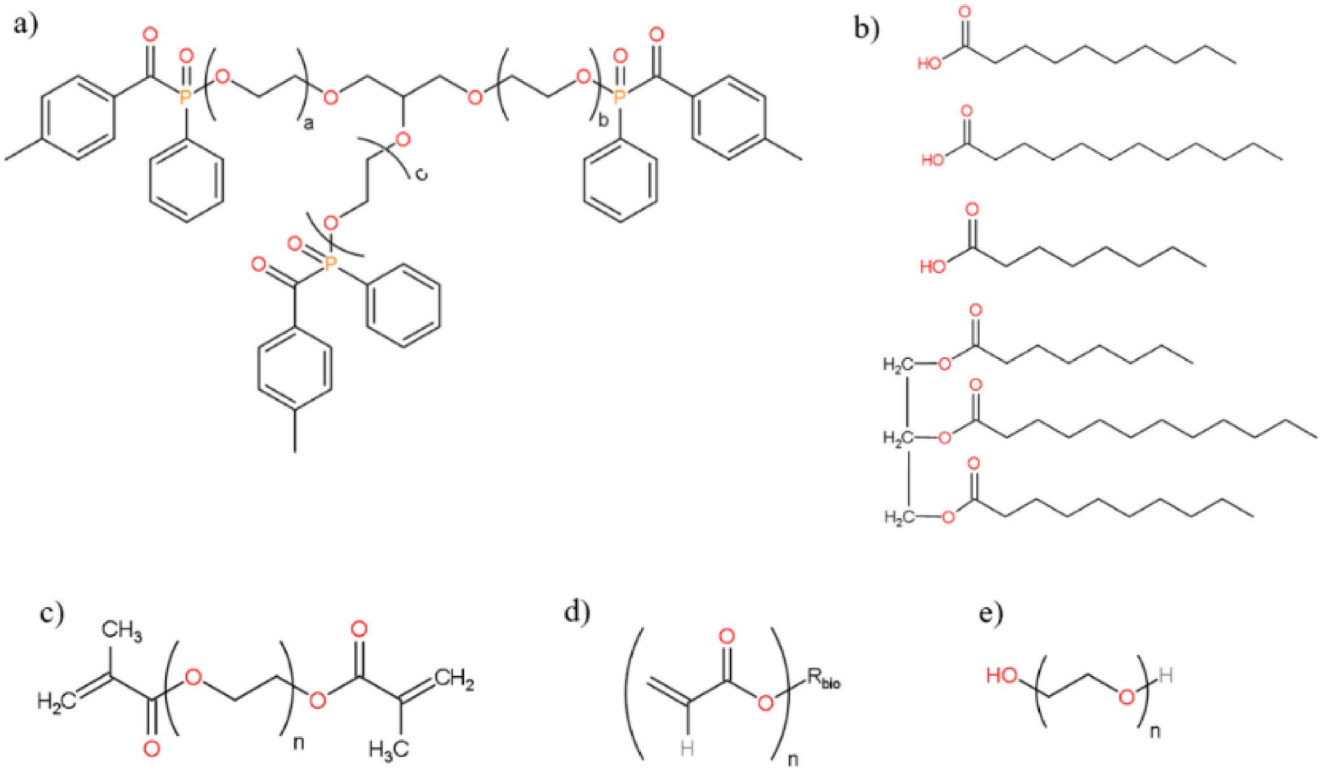

Fig. 1 Structure of the (**a**) Polymeric photo initiator (**b**) Coconut oil (**c**) Polyethylene Glycol (200) di methacrylate (**d**) Fatty Acid Modified Polyester Acrylate (**e**) PEG

Table 1 Formulation of the biobased photopolymers

Material	BP-1 (%)	BP-2 (%)
Fatty Acid Modified Polyester Acrylate S7201	38.70	38.70
Fatty Acid Modified Polyester Acrylate S7202	23.00	23.00
Polyethylene Glycol Di Methacrylate S6201	38.30	38.30
Coconut Oil	30.00	-
PEG	-	30.00
Polymeric Photoinitiator	3.10	3.10

porous structures in the model obtained from the 3D printer through appropriate washing methods, and at the same time, increases the biodegradability of the scaffolds. The aim here is to create a scaffold model with a photopolymer resin in a 3D printer and to remove the structure that does not participate in the cross-linked network from this scaffold, thereby obtaining a biocompatible scaffold model suitable for the three-dimensional dispersion and proliferation of cells to be added to the porous scaffolds. Thus, the possibility of cell adhesion and growth on the scaffold will increase [18]. Table 1 presents the formulation of the bio-based photopolymer resin. A polymeric photoinitiator was used in an amount equal to 3.10% by weight of the active group that will participate in the polymerization.

The formulations given in Table 1 were added to a glass beaker and mixed at room temperature for half an hour using a mechanical stirrer with a three-blade shaft. After the mixing process, the amber-colored semi-viscous photopolymer resins were allowed to stand at room temperature for half an hour to allow air bubbles to escape.

2.3. Parameter Selection

A critical factor in developing photopolymers for 3D printing is the resin's sensitivity to UV light. Excessive UV light absorption can lead to over-curing of the 50-micron (determined layer thickness) layers, compromising the precision of the 3D printed object. To mitigate this issue, we investigated the curing behavior of our biobased photopolymer resin using Photo-DSC [19].

A DSC 300 Select (Netzsch, Mannheim, Germany) equipped with an OmniCure®S2000 UV-curing spot system (Lumen Dynamics, Toronto, ON, Canada) was used for photo-curing experiments conducted isothermally at 35 °C under a nitrogen atmosphere. A high-pressure mercury short arc lamp with a maximum intensity of 100 W/cm², emitting primarily between 320 and 500 nm, served as the light source.

The experimental determination of the 100% curing degree of the formulations was achieved by relating the heat of reaction measured at time t (180 s) under a constant nitrogen flow of 20 ml/min, a constant temperature of 35 °C, and a light intensity of 90 W/cm² to the total heat of reaction (ΔH_{total}) measured after the heat flux reached a steady state [20].

Table 2 Properties analysis results for different light intensities for BP-1 and BP-2 formulations

Formulation	Light Intensity (W/cm^2)	ΔH (J/g)	Exposure Time (s)	Curing Degree (%)
BP-1	30	200.00	6	66.67
	45	204.00	6	68.00
BP-2	30	196.70	6	65.57
	45	243.70	6	81.23

2.3.1. UV Light Intensity

Shallow, open aluminum pans were filled with a 1.5 mg droplet of the mixed sample (resulting in a thickness of approximately 50 micrometer (μm) and placed in a cell for UV experiments. Experiments were conducted under a nitrogen atmosphere at a flow rate of 20 ml/min and a temperature of 35 °C, using light intensities of 30 and 45 W/cm². The exposure time was fixed at 6 s for all experiments. The measurement results for BP-1 and BP-2 formulations are presented in Table 2; Fig. 2.

2.3.2. Exposure Time

Shallow, open aluminum pans were filled with a 1.5 mg droplet of the mixed sample (resulting in a thickness of approximately 50 μm) and placed in a cell for UV experiments. Experiments were conducted for 13 s at 35 °C under a nitrogen atmosphere with a flow rate of 20 ml/min. The UV light intensity was kept constant at 45 W/cm² for these experiments. The performance of the materials under these conditions is shown in Table 3; Fig. 3.

Based on preliminary studies, Photo-DSC analysis was used to identify the conditions necessary to achieve a curing conversion exceeding 85%. The targeted 85% curing conversion was determined as a critical threshold for optimal tissue scaffold formation during the 3D printing process. When parameters with lower curing conversions were used, 3D tissue scaffolds with poor structural integrity and non-functionality were obtained. Guided by these results, print optimization for both resin formulations were carried out on a 3D printer utilizing a 385 nm light source. The printing process was conducted under controlled conditions of 45 W/cm² power density and a constant temperature of 35 °C, with an exposure time of 13 s per 50 μm layer.

2.4. 3D Printing

A Sega 120 (3bfab Teknoloji A.Ş., Türkiye) 3D printer, operating on the DLP-based curing principle with a wavelength

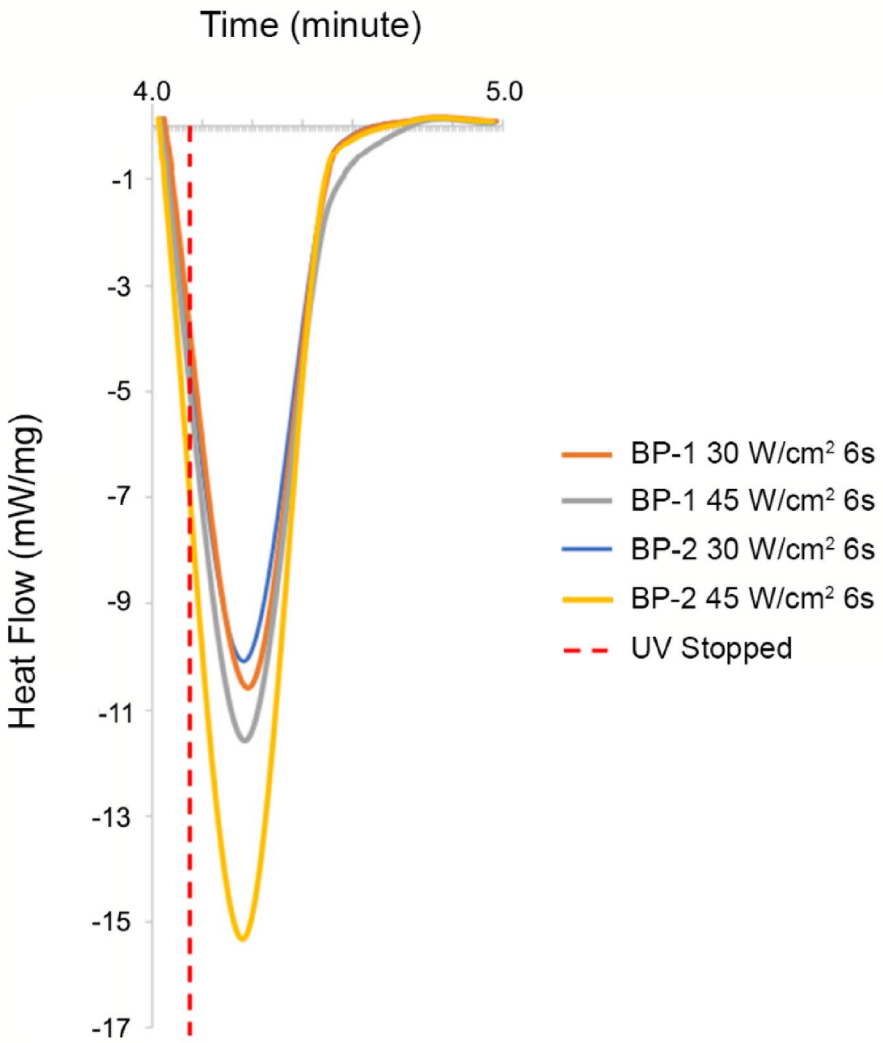

Fig. 2 Enthalpy analysis of BP-1 and BP-2 formulations exposed to different light intensities for 6 s

Table 3 Properties analysis results for different exposure times for BP-1 and BP-2 formulations

Formulation	Light Intensity (W/cm^2)	ΔH (J/g)	Exposure Time (s)	Curing Degree (%)
BP-1	45	257.00	13	85.67
BP-2	45	298.60	13	99.53

of 385 nm, was used for the study. Since the original print bed and resin tank of the 3D printer were too large for the desired models, they caused drops effects during printing. Therefore, the revisions shown in Fig. 4 were made to the print bed and resin tank. The resin tank was made of highly transparent glass and its surface in contact with the resin was coated with silicone. This silicone surface, thanks to its non-stick property, will allow the cured resin to be easily separated from the surface. In addition, the surface of the aluminum print bed was roughened by laser treatment to increase the adhesion behavior of the print to the print bed. The schematic diagrams and dimensions of the 3D printed parts are shown in Fig. 5.

To ensure that the support structures adhered well to the print bed, the first 40 layers, each with a thickness of 50 microns (totaling 2 mm), were cured for 36 s under a UV light intensity of 90 W/cm². The main layers, each with a thickness of 50 microns, which would form the scaffold structure, were cured for 13 s under a UV light intensity of 45 W/cm². To obtain thin and delicate models in the scaffold structure, the print bed, which moves along the z-axis of the 3D printer, was programmed to move very slowly during the 3D printing process. After curing the 50-micron layer

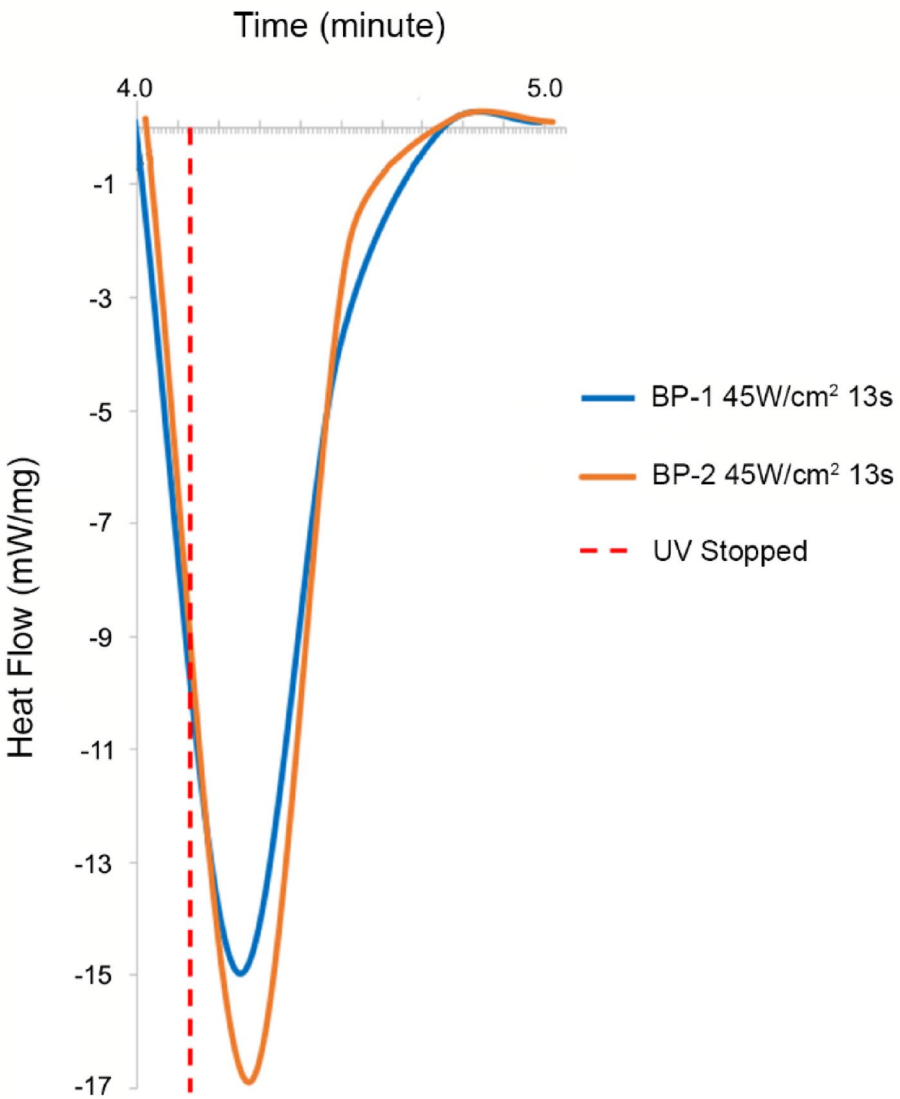

Fig. 3 Enthalpy analysis of BP-1 and BP-2 formulations exposed to 13 s of light at an intensity of 45 W/cm²

on the bottom of the resin tank, the print bed was raised 0.5 mm in 3 s, and then another 0.5 mm in 3 s, for a total of 1 mm, in two stages. The descent of the print bed to a thickness of 50 microns to cure the next layer thickness was set to take 3 s. The temperature of the resin was kept constant at 35 degrees Celsius throughout the entire printing process. The image of the 3D print obtained under these conditions is given in Fig. 6a.

2.5. Samples Drying and Post Process

The models obtained from the 3D printer were gently washed with ethyl alcohol to remove unreacted resin (Fig. 6b). the prints on the print bed were separated with a sterile scalpel and placed in a beaker containing ethyl alcohol placed in an ultrasonic bath. After 3 min, the dirty alcohol was removed and replaced with fresh alcohol, and the beaker was placed back in the ultrasonic bath. This process was repeated 3 times. After that, the prints were removed from the beaker and carefully placed in a Petri dish. The Petri dish containing the prints was placed in an oven at 60 degrees Celsius and dried for half an hour. After half an hour, the prints in the Petri dish were placed in a UV cabinet operating at a wavelength of 300–500 nm and cured for 10 min for post-processing. After all these processes, the obtained scaffolds were stored in a closed Petri dish in the refrigerator until cell culture studies. The scaffolds obtained from BP-1 resin were named BP-1sld (Fig. 6c), and those obtained from BP-2 resin were named BP-2sld (Fig. 6d).

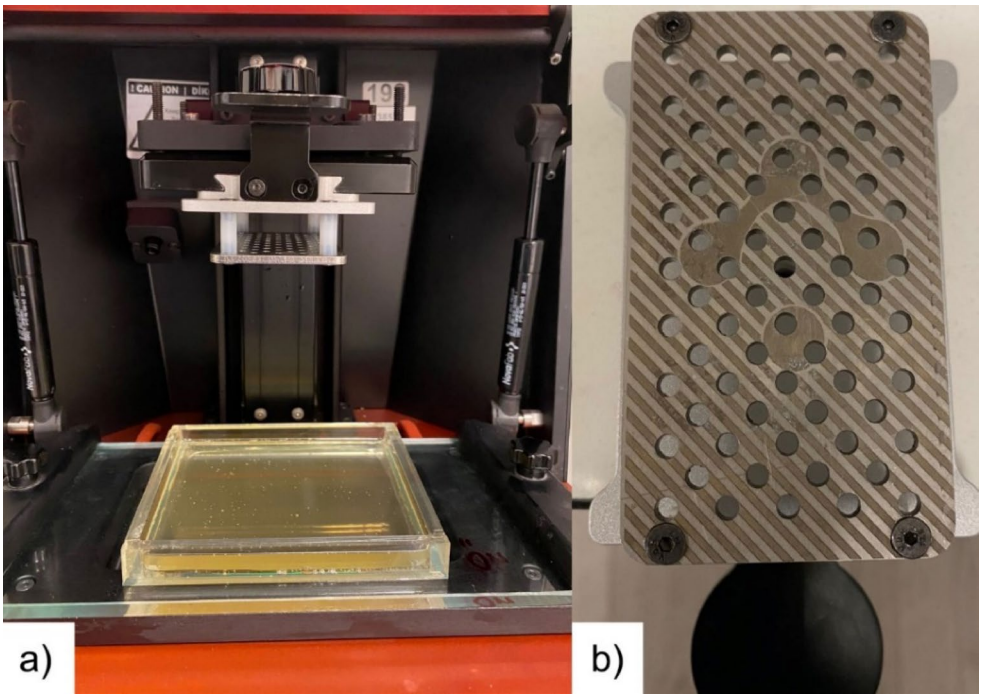

Fig. 4 Modifications made to the 3D printer: (**a**) The dimensions of the glass resin tank with a silicone bottom have been reduced as shown in the figure. (**b**) The dimensions of the print bed have been adjusted to match those of the resin tank (12 cm x 6 cm)

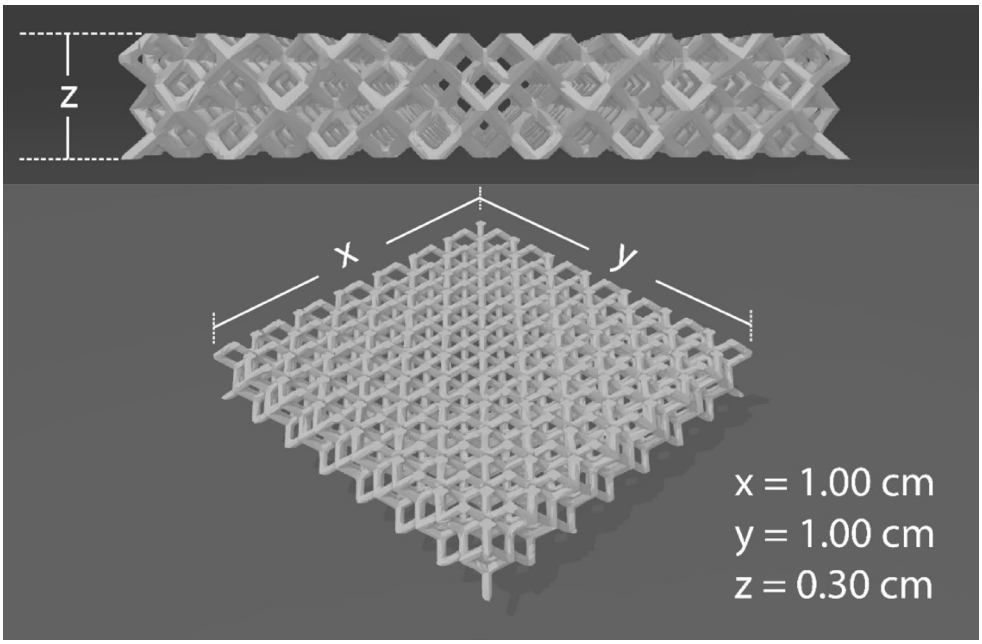

Fig. 5 Dimensions of the scaffold to be obtained from BP-1 and BP-2 formulations in the x, y, and z axes

2.6. Characterization

2.6.1. ATR-FTIR

The chemical composition and functional groups of BP-1, BP-2 resin formulation and BP-1sld and BP-2sld scaffolds, were determined by Bruker Alpha, Bruker Scientific Instrument, Billerica, MA in the wavelength range of 4000–500 cm^{-1}.

2.6.2. In-situ Degradation in PBS

The in-situ degradation of BP-1sld and BP-2sld scaffolds was conducted in a 15 mL PBS (phosphate-buffered saline) solution at 24 degrees Celsius and pH 7.4. Samples were placed in bottles containing 15 mL of PBS solution and kept under atmospheric conditions for 21 days [21].

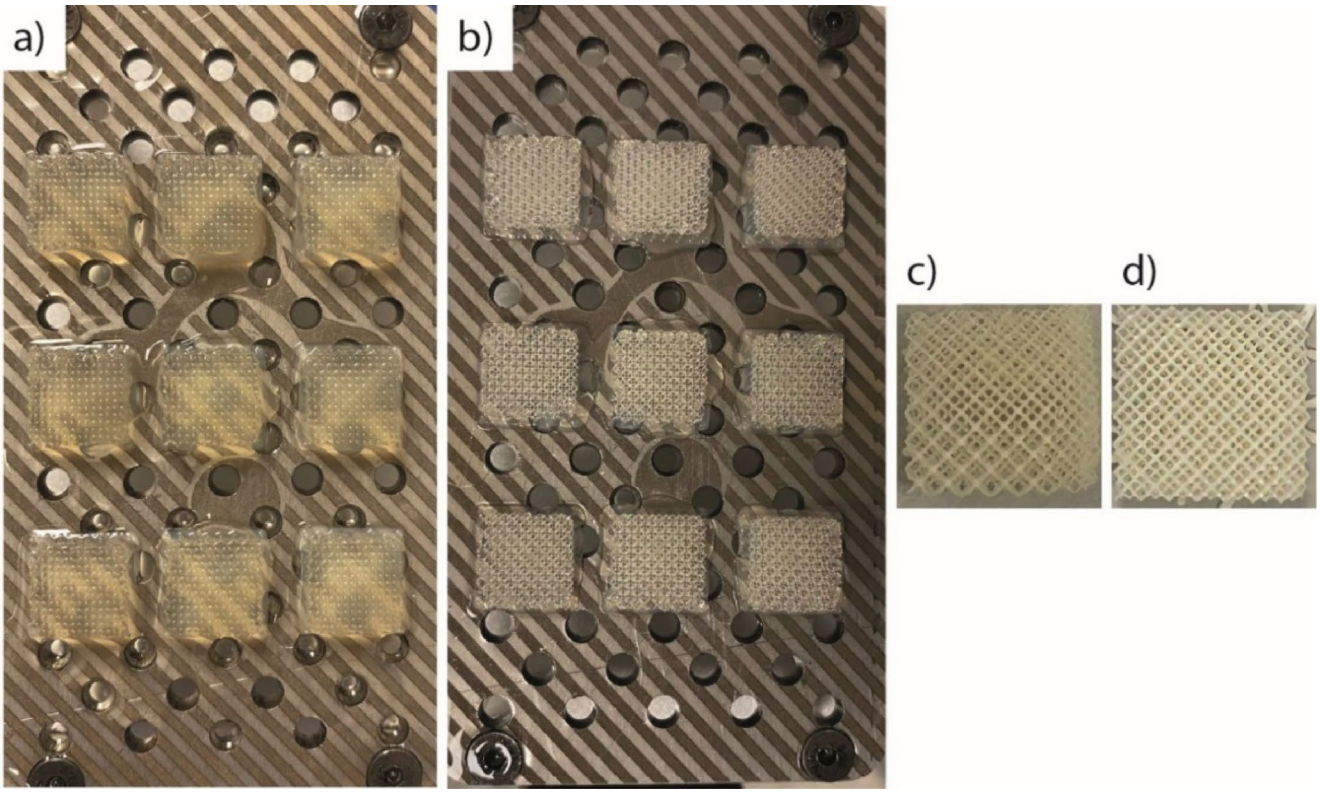

Fig. 6 (**a**) Image of the scaffolds obtained from the 3D printer. (**b**) Image of the scaffolds after gentle washing with ethyl alcohol. (**c**) Image of the BP-1sld scaffold after the washing process. (**d**) Image of the BP-2sld scaffold after the washing process

2.7. Biocompatibility Assessments

The L929 mouse fibroblast cell line (ATCC CCL-1) was used in cytotoxicity assays as well as for evaluating cellular attachment and proliferation on scaffolds. The cells were cultured in DMEM (Dulbecco's Modified Eagle Medium) supplemented with 10% fetal bovine serum (FBS) and 1% Penicillin-Streptomycin at 37 °C in a humidified incubator with 5% CO_2. The medium was refreshed every 2–3 days. When the cells reached 70% confluency, they were split at a ratio of 1:4 to 1:8.

2.8. Extraction Process of Scaffolds and their Cytotoxicity Effects

The extraction process for testing scaffold biocompatibility was performed in accordance with ISO 10993-12. To achieve a 200% extraction ratio, medium containing 6 cm^2/mL of scaffolds was incubated at 37 °C for 24 h as recommended (ISO 10993-12:2021, 2021).

Cell viability was assessed using the MTT (3-[4,5-dimethylthiazol-2-yl]-2,5-diphenyl tetrazolium bromide) assay. Briefly, cells were seeded into 96-well plates at a density of 1×10^4 cells/well and allowed to adhere overnight. The cells were treated with extracts at concentrations ranging from 25 to 100% for 24 h. Following treatment, MTT solution (1 mg/mL in medium) was added to each well and incubated for 3–4 h at 37 °C. The resulting formazan crystals were dissolved in 100 µL of DMSO, and absorbance was measured at 570 nm using a microplate reader (Infinite F200 Pro Microplate Reader, TECAN AG, Switzerland). Cell viability was expressed as a percentage relative to the untreated control group (ISO 10993-5:2009, 2009).

2.9. Evaluation of Cell Attachment and Proliferation on Scaffolds

To test cell attachment and proliferation on the scaffolds, the scaffolds were sterilized with EtOH and UV, followed by the addition of 5×10^5 cells to each scaffold (approximately 1 mm^3). The scaffolds were sterilized with 70% EtOH for 1 h, followed by UV sterilization for 15 min on both sides.

To prevent cell attachment to the petri dish and promote attachment to the scaffolds, the petri dish was coated with PDMS (Polydimethylsiloxane). After washing the scaffolds with PBS, 5×10^5 cells were seeded onto each scaffold (approximately 1 mm^3) in a small volume of medium. After 3 h, the wells were filled with medium.

The following day, the scaffolds were washed with PBS, transferred to a clean well, and cell proliferation was

evaluated using the CCK-8 assay on days 1, 3, 5, and 7 [22]. The cells were incubated with medium containing 10% CCK-8 solution for 3–4 h, and the absorbance at 570 nm was measured to assess the color change. As a positive control, a well from a 24-well plate with known cell count at 100% confluence was used. At the end of the incubation period, the cells were fixed with cold 4% PFA for 15 min after PBS washing and then prepared for scanning electron microscopy (SEM).

2.10. Scanning Electron Microscope (SEM)

Scaffold samples were cut into half at the middle z-axis by lancet to take images from the center of the samples. Samples underwent sequential ethanol dehydration with 35%, 50%, 70%, 80%, 90%, and 95% (v/v) ethanol washes for 10 min each. A final incubation in 100% ethanol for 15 min was performed to ensure complete removal of water content.

Hexamethyldisilazane (HMDS) solutions were prepared in ethanol, and samples were incubated for 10 min in each solution at 50%, 60%, 70%, 80%, and 90%. Finally, 100% HMDS was applied, and the samples were left to dry overnight with the well-plate lid slightly open to allow for HMDS evaporation. The dried samples were mounted onto aluminum stubs using conductive carbon tape and sputter-coated with an Au/Pd layer (3.5 nm thickness) using a Cressington 108 Sputter Coater (40 mA for 120 s). SEM micrographs were acquired using a Zeiss/Leo Supra VP35 at magnifications of 65x, 500x, and 1500x, with an acceleration voltage of 3 kV.

3. Result and Discussion

3.1. Effects of UV Light Intensity and Exposure time on the Enthalpy and Curing Degree

Upon examining the data presented in Table 2; Figs. 2, it becomes apparent that augmenting the UV intensity from 30 to 45 W/cm² induced a pronounced escalation in the energy of BP-2, in contrast to a more subdued response in BP-1. This disparity in energy absorption directly correlated with a substantial enhancement in the curing conversion of BP-2, reaching a maximum of 81%. Subsequent experiments, wherein the exposure time was extended to 13 s at a fixed intensity of 45 W/cm² (as illustrated in Table 3; Figs. 3), demonstrated a marked increase in the energy released by both formulations. Consequently, the curing conversion of BP-1 attained 85.67%, while that of BP-2 reached an impressive 99.53%. The differential behavior of the two formulations, despite their shared base components, can be attributed to the distinct roles of coconut oil and PEG. The comparatively large molecular volume of coconut oil in BP-1 hindered the penetration of UV radiation into the resin matrix, whereas the PEG in BP-2 underwent partial photodegradation, serving as a hydrogen donor and thereby facilitating the curing reaction [23, 24].

3.2. ATR-FTIR

Figure 7 presents the FTIR spectra of BP-1 and BP-2 photopolymers, as well as BP-1sld and BP-2sld scaffolds. The spectra of the photopolymers exhibit a characteristic C=C double bond stretching vibration at 1630 cm^{-1}, typical of acrylates. Furthermore, O-CH_2 bending and strong C-O-C stretching vibrations are observed at 1407, 1295, and 1163 cm^{-1}. In the BP-2 liquid photopolymer spectrum, broad O-H bands originating from PEG are detected between 3600 and 3200 cm^{-1}. For the 3D printed and washed scaffolds, the C=C double bond stretching vibration at 1630 cm^{-1} vanishes. The intense O-H bands from PEG are absent in the BP-2sld spectrum. Both resin spectra display a peak at 1725 cm^{-1}, attributed to the C=O groups within the resin chains [25]. The results show that 3D prints obtained with optimized parameters were cured successfully.

3.3 Cytocompatibility of the Scaffolds

3.3.1. Swelling and Degradation Behavior of the Scaffolds

After the washing process, BP-1sld and BP-2sld scaffolds were placed in separate glass containers containing 15 ml of PBS solution, and their degradation behaviors were monitored at room temperature for 3 weeks. Weight changes were precisely measured on days 1, 3, 6, 8, 14, and 21. On the first day, a slight mass loss was observed in the BP-1sld scaffold, while a more significant decrease was recorded in the BP-2sld scaffold. This is attributed to the leaching of trace amounts of coconut oil from the porous structure of BP-1sld and the leaching of free PEG molecules from the porous structure of BP-2sld into the PBS solution, resulting in mass loss.

On the sixth day, both scaffolds exhibited weight gain; 32% in BP-1sld and 26% in BP-2sld. This increase is associated with the penetration of PBS solution into the porous structure of the scaffolds. On the eighth day, a 20% weight loss occurred in the BP-1sld scaffold, while the decrease in BP-2sld was only 2%. Additionally, it was observed that a portion of the BP-1sld scaffold gradually detached, resulting in the void shown in Fig. 8b. The rapid abatement of BP-1sld on the eighth day, following the rapid swelling observed on the sixth day, has led to the disruption of its structural integrity [26].

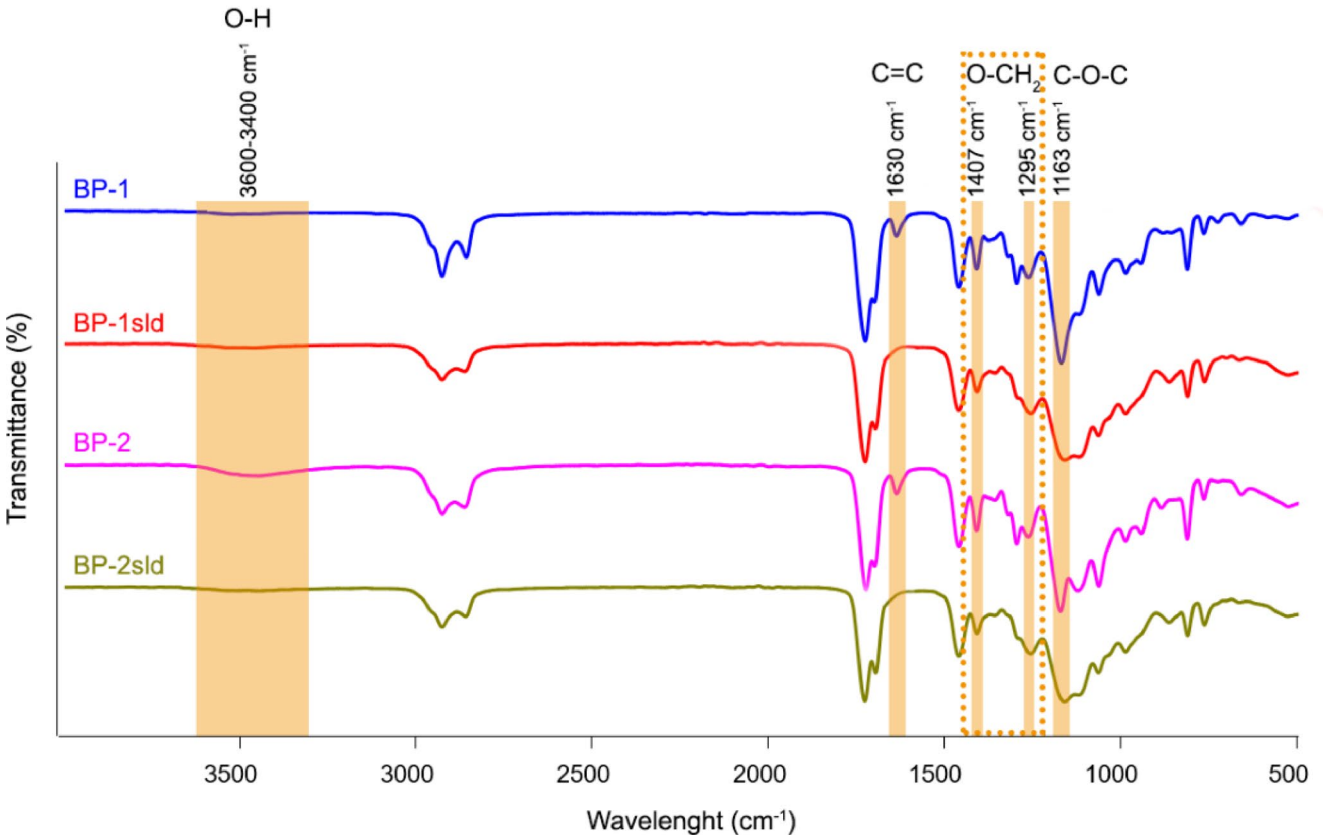

Fig. 7 FTIR spectra of BP-1, BP-2 resin formulations and BP-1sld, BP-2sld scaffolds

On the twenty-first day, the final day of the experiment, the BP-1sld scaffold lost 6% of its initial weight, while the BP-2sld scaffold lost 16% and assumed the final appearance shown in Fig. 8b. At the end of 21 days, BP-1sld scaffolds showed significant degradation in the PBS solution, whereas BP-2sld scaffolds maintained their structural integrity. These results indicate that BP-2sld scaffolds exhibited a more stable degradation profile in PBS solution and maintained their structural integrity for a longer duration.

3.3.2. Cell Population Assessment

Cell population studies were conducted with L-929 cells for 24 h at four different concentrations: 12.5%, 25%, 50%, and 100%. Measurements were performed in three biological replicates, and the average of these replicates is shown in the graph in Fig. 9. As seen in Fig. 9a, extracts obtained from BP-1sld and BP-2sld scaffolds and their doses did not exhibit any toxic effects on the L-929 cell line, exceeding the minimum 80% viability limit [27]. These results demonstrate that both scaffolds provide a biocompatible and non-toxic environment for cells. These findings suggest that the scaffolds support cell viability and are potentially safe for tissue engineering applications.

As seen in Fig. 9b, it was determined through CCK-8 proliferation assay that L929 cells adhered to and proliferated on BP-1sld. Although cell adhesion was observed on BP-2sld, no proliferation was detected in the following days. The higher cell proliferation was observed on BP-1sld in 7 days. These results demonstrate that BP-1sld scaffolds provide a suitable environment for both the adhesion and proliferation of L929 cells. While cell adhesion was observed in BP-2sld scaffolds, a significant proliferation process was not detected in the following days. The high cell proliferation rate observed in BP-1sld scaffolds indicates that these scaffolds are a promising candidate for tissue engineering applications. Particularly, BP-1sld scaffolds may be more suitable for tissue types where cell proliferation needs to be supported. However, the reasons for the lack of proliferation in BP-2sld scaffolds and the effects of this situation on tissue engineering applications require further investigation. These findings are important for understanding the effects of scaffolds on cell interactions. In our ongoing studies, we plan to evaluate the effects of these scaffolds on different cell types and their performance under in vivo conditions.

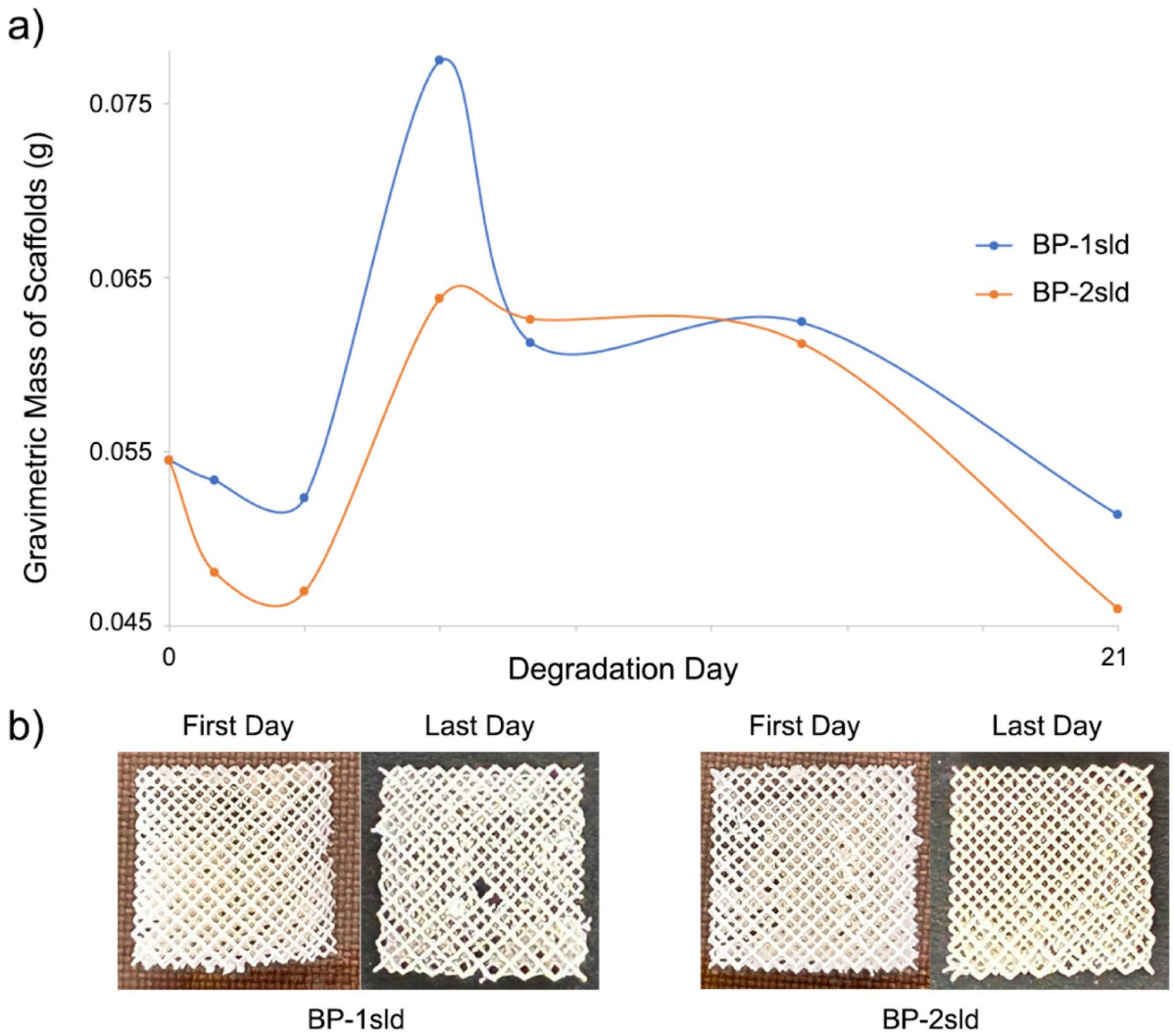

Fig. 8 (**a**) The weight variation and (**b**) The visual transformation of BP-1sld and BP-2sld scaffolds over a 21-day period

3.3.3. Imaging of Cells on Scaffolds

Figure 10 presents SEM images revealing that cells retained their fusiform shape and exhibited strong adhesion to the scaffold surface. Importantly, the micrographs of BP-1sld and BP-2sld are consistent with the results obtained from the CCK-8 assay (7th day). These SEM images confirm that the cells successfully adhered to the scaffold surface and maintained their natural morphologies. The preservation of the cells' fusiform shape indicates that the cells are viable and healthy. This supports the notion that the scaffolds provide a suitable environment for cells and are potentially safe for tissue engineering applications.

The consistency between the cell proliferation results obtained from the CCK-8 assay and the SEM images enhances the reliability and validity of our findings. The high cell proliferation observed in BP-1sld scaffolds is supported by the dense adhesion and spreading of cells on the scaffold surface in the SEM images. Conversely, the low proliferation observed in BP-2sld scaffolds in the CCK-8 assay is consistent with the fewer cells adhering and spreading in the SEM images.

These data are crucial for understanding the effects of scaffolds on cell interactions and tissue formation. In our ongoing studies, we plan to evaluate the effects of these scaffolds on different cell types and their performance under in vivo conditions. These evaluations will help us determine the suitability of the scaffolds for tissue engineering applications more comprehensively.

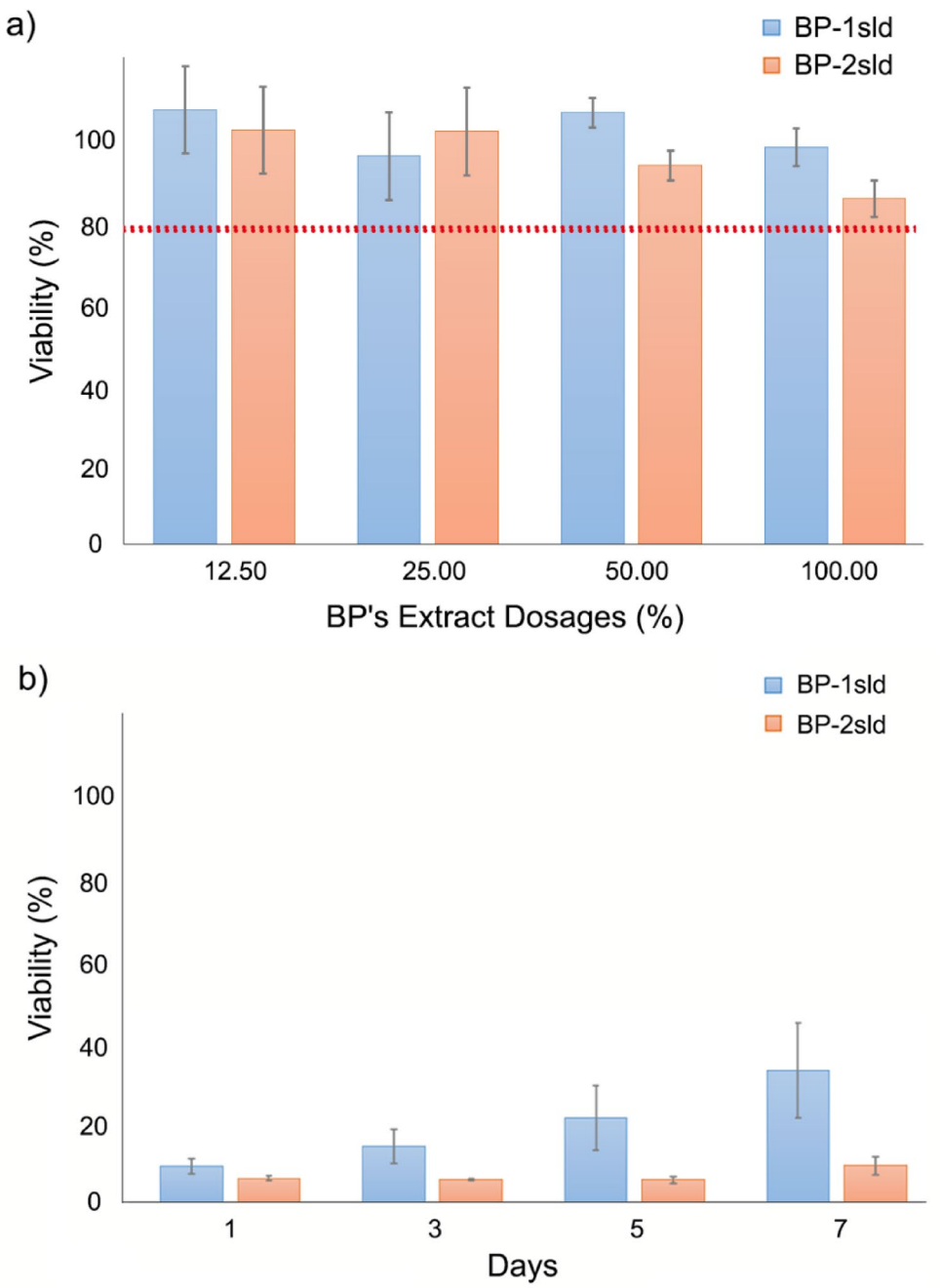

Fig. 9 (**a**) Relative cell population over 24 h at different concentrations (**b**) The viability/proliferation of cells attached to scaffolds over 7 days

4. Conclusions

In this study, photopolymer resin formulations containing acrylate oligomers and monomers derived from bio-based resources, using an eco-friendly and sustainable approach, were developed. These formulations, enhanced with coconut oil or polyethylene glycol (PEG), offer innovative and sustainable solutions for tissue engineering applications. Optimal curing conditions for the DLP-based 3D printer were successfully determined using a Photo-DSC device, in line with the principles of resource efficiency and waste minimization. Tissue scaffolds with a layer thickness of 50 µm were produced using the DLP 3D printing method under optimized conditions such as 45 W/cm² light intensity, 35 °C, and 13 s of UV exposure per layer, utilizing two separate photopolymer resin formulations containing coconut oil (BP-1) and PEG (BP-2), respectively.

The relatively large molecular volume of coconut oil in the BP-1 formulation partially hindered the penetration of UV radiation into the resin matrix, resulting in slightly lower curing. However, compared to BP-2, it facilitated increased porosity in the scaffold after washing and post-processing,

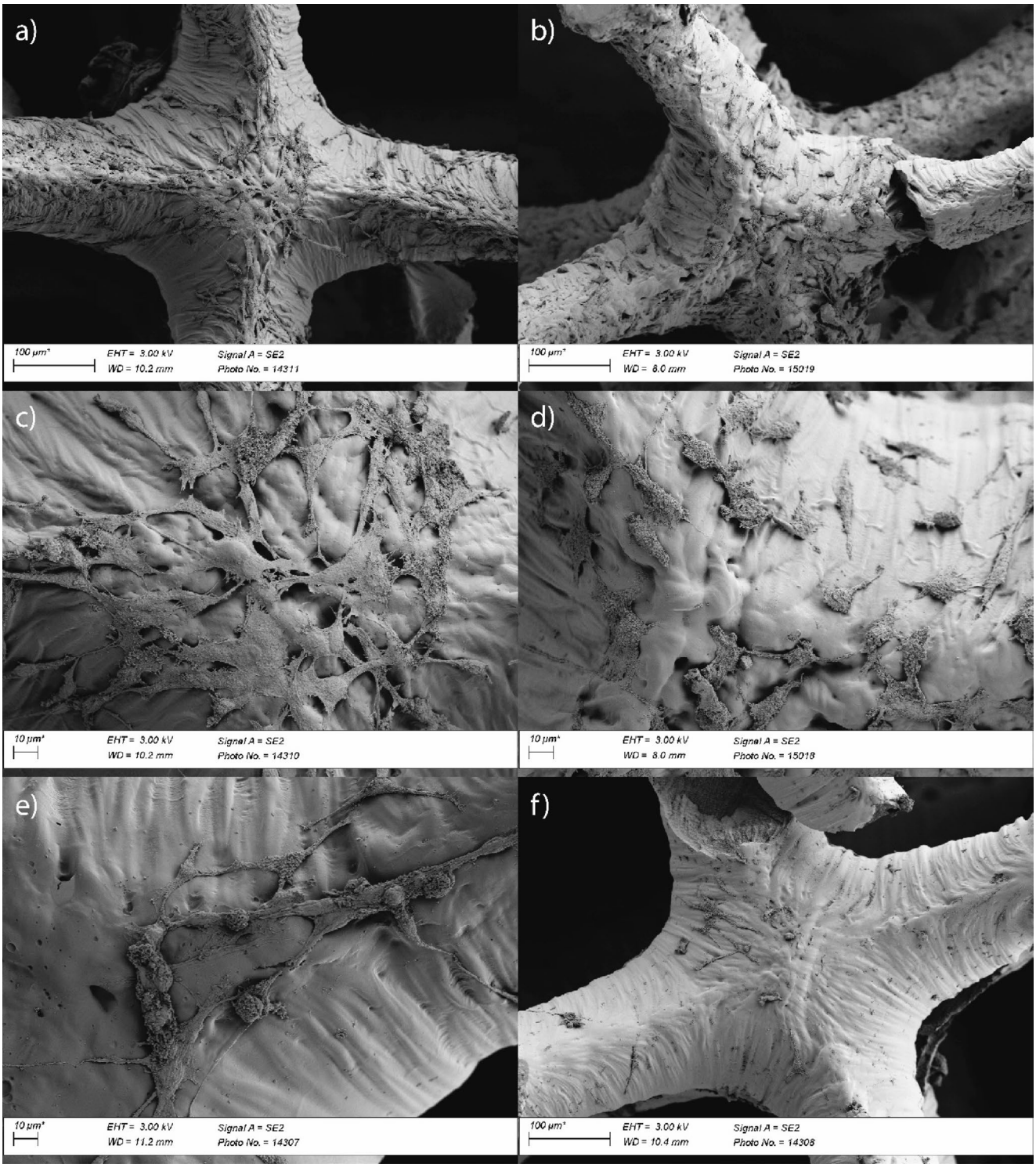

Fig. 10 SEM images depict L-929 cells seeded on bioprinted BP-1sld (**a-d**) and BP-2sld (**e-f**) cross-linked networks attached to BP scaffolds. Images **a**, **b**, **f** are magnified 500x, while **c**, **d**, and **e** are magnified 1500x

thereby promoting cell adhesion and tissue formation. This situation highlights the balance between biocompatibility and environmental sustainability. Both photopolymer resin formulations developed in the study, in conjunction with the compatible DLP-based 3D printer, offer eco-friendly and sustainable new perspectives for tissue engineering applications.

The results obtained demonstrate that these bio-based photopolymer resin formulations and DLP-based 3D printing technology have sustainable and promising potential for tissue engineering applications. In particular, BP-1 scaffolds may be suitable for tissue types where cell proliferation needs to be supported, while BP-2 scaffolds may be more suitable for applications requiring long-term structural integrity. This study is an important step towards the development of sustainable tissue engineering solutions.

Supplementary Information The online version contains supplementary material available at https://doi.org/10.1007/s10924-025-03592-7.

Acknowledgements This work was supported by 3BFAB Teknoloji A.Ş. and Kempropol Chemical and Polymer Substances and Industry Trade Inc. Istanbul/Türkiye.

Author Contributions Ö.T.: Conceptualization, Methodology, Writing-Original draft preparation, Writing- Reviewing and Editing, M.V.K.: Supervision, Conceptualization, Methodology, Writing-Original draft preparation, R.C.: Validation, Data curation, Formal analysis, A.A.: Conceptualization, Data curation, E.D.: Visualization, Methodology, S.Ç.: Conceptualization, Methodology, Writing-Original draft preparation.

Funding Open access funding provided by the Scientific and Technological Research Council of Türkiye (TÜBİTAK).

Data Availability No datasets were generated or analysed during the current study.

Declarations

Conflict of interest The authors declare no conflict of interest.

References

1. Briede S et al (2022) Acrylation of biomass: A review of synthesis process: Know-how and future application directions. Curr Opin Green Sustainable Chem 35:100626. https://doi.org/10.1016/j.cogsc.2022.100626
2. Liang B et al (2019) Synthesis and characterization of a novel tri-functional bio-based methacrylate Prepolymer from castor oil and its application in UV-curable coatings. Ind Crops Prod 135:170–178
3. Luo N, Ma G, Qu J (2024) Preparation of Rosin epoxy soybean oil acrylate with high bio-renewable carbon content for 3D printing. Ind Crops Prod 222:119622
4. Wu Y et al (2021) H-bonds and metal-ligand coordination-enabled manufacture of palm oil-based thermoplastic elastomers by photocuring 3D printing. Additive Manuf 47:102268
5. Javaid M et al (2022) 3D printing applications for healthcare research and development. Global Health J 6(4):217–226
6. Wu T et al (2024) Advancements in developing biomaterials for 3D printing photosensitive resins containing quaternary ammonium molecules for enhanced oral healthcare. Next Mater 4:100211
7. Perier-Metz C et al (2022) An in Silico model predicts the impact of scaffold design in large bone defect regeneration. Acta Biomater 145:329–341
8. Prem Ananth K, Jayram ND (2024) A comprehensive review of 3D printing techniques for biomaterial-based scaffold fabrication in bone tissue engineering. Annals 3D Print Med 13:p100141
9. Soltani Gerdefaramarzi R, Ebrahimian-Hosseinabadi M, Khodaei M (2024) 3D printed poly(lactic acid)/poly(ε-caprolactone)/graphene nanocomposite scaffolds for peripheral nerve tissue engineering. Arab J Chem 17(9):105927
10. Wang W et al (2024) Two-photon polymerization-based 3D microscaffolds toward biomedical devices. Chem Eng J 493:152469
11. Jeong YG et al (2024) 3D digital light process bioprinting: Cutting-edge platforms for resolution of organ fabrication. Mater Today Bio 29:101284
12. Junyi Zhou XA, Ibrahim A (2019) Xiaoxuan Liu., *Progress in the development of polymeric and multifunctional photoinitiators.* Progress in Polymer Science, 99: p. 101165
13. Wang Z et al (2024) Digital light processing of customized elastic scaffolds by efficient thiol-yne crosslinking. Eur Polymer J 202:112586
14. Tan LJ, Zhu W, Zhou K (2020) Recent progress on polymer materials for additive manufacturing. Adv Funct Mater, 30(43)
15. Yang X et al (2024) Low-temperature DLP 3D printing of low-concentration collagen methacryloyl for the fabrication of durable and bioactive personalized scaffolds. Chem Eng J 497:155650
16. Han Y et al (2024) A 3D printable gelatin Methacryloyl/chitosan hydrogel assembled with conductive PEDOT for neural tissue engineering. Compos Part B: Eng 273:111241
17. Lago MA et al (2015) Photoinitiators: a food safety review. Food Addit Contam Part Chem Anal Control Expo Risk Assess 32(5):779–798
18. Kuzina MA et al (2023) 3D-Printed inherently porous structures with tetrahedral lattice architecture: experimental and computational study of their mechanical behavior. Macromol Mater Eng 308(9):2300041. https://doi.org/10.1002/mame.202300041
19. Bakhshi H et al (2022) Photo-Curing kinetics of 3D-Printing Photo-Inks based on Urethane-Acrylates. Polym (Basel) 14(15):2974. https://doi.org/10.3390/polym14152974
20. Jiang F, Drummer D (2020) Curing kinetic analysis of acrylate photopolymer for additive manufacturing by Photo-DSC. Polym (Basel) 12(5):1080. https://doi.org/10.3390/polym12051080
21. Wu L, Ding J (2004) Vitro degradation of three-dimensional porous poly(D,L-lactide-co-glycolide) scaffolds for tissue engineering. Biomaterials 25(27):5821–5830
22. Lv D et al (2016) A three-dimensional collagen scaffold cell culture system for screening anti-glioma therapeutics. Oncotarget 7(35):56904
23. Sionkowska A (2006) The influence of UV light on collagen/poly(ethylene glycol) blends. Polym Degrad Stab 91(2):305–312

24. Tasdelen MA, Moszner N, Yagci Y (2009) The use of poly(ethylene oxide) as hydrogen donor in type II photoinitiated free radical polymerization. Polym Bull 63(2):173–183
25. Mondal D et al (2021) Acrylated epoxidized soybean oil/hydroxyapatite-based nanocomposite scaffolds prepared by additive manufacturing for bone tissue engineering. Mater Sci Eng C Mater Biol Appl 118:111400
26. Fayyazbakhsh F, Khayat MJ, Leu MC (2022) *3D-Printed Gelatin-Alginate Hydrogel Dressings for Burn Wound Healing: A Comprehensive Study.* Int J Bioprint, 8(4): p. 618
27. Segeritz C-P, Vallier L (2017) Chapter 9–Cell Cult ure: growing cells as model system in vitro, In: Morteza Jalalli, Francesca Y. L. Saldanha, Mehdi Jalali (eds)Basic science mothds for clinical researchers, Academic press, p. 151–172 ISBN 9780128030776. https://doi.org/10.1016/B978-0-12-803077-6.00009-6